SciMedCentral

Annals of Vascular Medicine & Research

Review Article

Intra-Myocardial Arteriolar Architecture Impact on Vulnerability of Sub-Endocardium to Ischemia

Ritman EL*

Department of Physiology and Bioengineering Mayo Foundation College of Medicine, USA

***Corresponding author**

Erik L Ritman, Department of Physiology and Bioengineering Mayo Foundation College of Medicine, Emeritus Office Mayo Clinic Rochester Minnesota, 55905, USA, Email: elran@mayo.edu

Submitted: 14 March 2022

Accepted: 07 May 2022

Published: 10 May 2022

ISSN: 2378-9344

Keywords

- Trans-myocardial perfusion intra-myocardial arterioles; Myocardial arteriolar transit times; Myocardial Contraction

Abstract

This overview of direct measurement and 3D micro-CT image data to measure transmural distribution of myocardial perfusion, compression arterial branching geometry and the transmural locations of the terminal arterioles. From those data, blood flow, flow transit times to those terminal arterioles and their transmural locations were estimated. Several putative regional intra-myocardial compression due to myocardial contraction are shown to combine with the micro-CT derived data to result in a transmural perfusion gradient and their impact on the vulnerability of that perfusion to sub-endocardial myocardium. This analysis addresses the interplaying roles of the following:

1) The branching geometry of the intra-myocardial arteriolar microcirculation and distribution of myocardial terminal arterioles.

2) The transmural distribution of intra-myocardial compression.

3) Interplay of the myocardial electro-mechanical activation, contraction and perfusion sequences within a single cardiac cycle.

ABBREVIATIONS

F: Perfusion; P: Blood Pressure; L: length of inter-branch arteriolar segment; D: Diameter of inter-branch arteriolar segment; TT: Transit time of blood flow from epicardial to terminal arteriole; R_o: Radius from center of left ventricular chamber to epicardial surface; R_i: Radius from chamber center to endocardial surface; S_c: Intra-myocardial stress in circumferential direction; S_t: Intra-myocardial stress in transmural direction

INTRODUCTION

Micro-CT provides high spatial resolution structural information of the three dimensional, intact, branching structures of arterial trees and their surrounding myocardial geometry within intact myocardial specimens. The ratio of the left ventricular walls' sub-endocardial to sub-epicardial perfusion has been demonstrated to be approximately 1.2 to 1.3 under resting conditions and to be somewhat less than 1.0 during severe exercise [1-3]. Despite this increased perfusion in the sub-endocardial region, preferential myocardial infarction in the sub-endocardium [4] occurs under various conditions such as epicardial coronary artery stenosis which restricts myocardial perfusion distal to the stenosis by virtue of reduced flow reserve [5] and reduced distal coronary arterial pressure [6]. An additional contribution to the vulnerability of the sub-endocardial myocardium is that it subjected to increasingly reduced time available for myocardial perfusion proportional to the reduced cardiac cycle durations at elevated heart rates.

Branching geometry of the intra-myocardial arteriolar microcirculation

As illustrated in Figure 1, the epicardial coronary arteries branch into small intramural arteries (approximately 0.5 – 1 mm lumen diameter) at regular intervals and at ninety degrees to the epicardial artery. Using histological and micro-CT imaging techniques applied to isolated pieces of myocardium, these branches precede transmurally to, broadly, one of three depths within the wall to terminate in terminal arterioles (ie less than 0.05 mm lumen diameter [9].

The branching pattern of these arteriolar trees changes from asymmetric "distributive" to a more equal "delivery" type as they progressively branch into smaller arterioles [10]. The arteriolar branches within these perfusion territories show minimal overlap with those in contiguous perfusion territories. The spatial density of arterioles of the order of 0.03 mm lumen diameter progressively increases from sub-epicardial to the sub-endocardial regions of the myocardial wall. At the sub-endocardium micro-embolization studies indicate 13 terminal arterioles/mm^3 [11] and direct visualization in micro-CT images indicates 9.5/mm^3 [9]. Thebesian vessels [12], which connect directly to the left ventricular chamber, range in diameter from 0.05 to 0.25 mm and hence were not included in the image-based estimates of intra-myocardial arterial density of terminal arterioles.

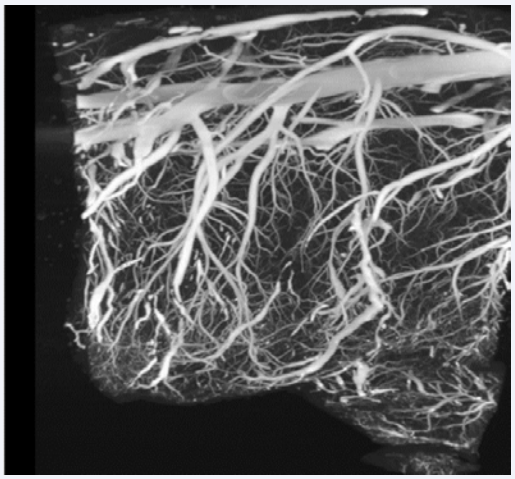

Figure 1 Micro CT image of opacified arterial tree within an adult pig's left ventricular wall (10 mm thick). Note that the transmural branches of the epicardial arteries follow a direct route towards the endocardium.

$$F = 417\ D^{3.01} \quad (1)$$

Arteriolar flow (F ml/g/min) through an arteriole of diameter D (cm) has been shown to be proportional the cube of the lumen diameter as [13]. Using this formula the flow in each terminal arteriole can be derived from the branching geometry of each intramural arteriolar tree within the isolated myocardial specimens [9]. This information, combined with the spatial density of the terminal arterioles, allows us to estimate the ratio of sub-endocardial to sub-epicardial myocardial perfusion. Those ratios (1.12–1.33) ,under resting conditions, correspond to those observed using radionuclide-based methods of estimating spatial distributions of myocardial perfusion in the myocardium of anesthetized experimental animals, which show those ratios to be 1.15 to 1.23 under resting conditions and 0.98 during hard exercise [1,2].

The arteriolar branching geometry results in the progressive decrease of intra-arteriolar blood pressure distal to the intramural arteriole's epicardial origin due to the progressively increasing vascular resistance along the arteriolar tree. By invoking Poisieulle's Law [14], the flow (F) in an arteriolar inter-branch segment diameter D and length L,

$$F \sim D^4(\Delta P/L) \quad (2)$$

where ΔP is the pressure gradient along the arteriolar segment

As we can estimate the flow (F) from the cubed lumen diameter and the sequential inter-branch lengths from the imaged intact arteriolar tree, then we can estimate the sequential vascular pressure drops along the pathway from the intramural arteriolar tree's origin at the epicardial coronary artery to one of the terminal arterioles from

$$\Sigma_i \Delta P[i] \sim F[i](L[i]/D^4[i]), \quad (3)$$

where i indicates the sequential location of each inter-branching along the origin-to-terminal arteriole pathway. In addition, using the fact that we can also calculate the luminal volume (V[i]) of an interbranch arteriolar segment i is:

$$V[i] = \pi D^2[i](L[i]/4) \quad (4)$$

along each inter-branch path, from its source at the epicardial coronary artery to each terminal arteriole, the transit time (TT) of blood flow from its epicardial coronary artery to each terminal arteriole's location along that flow path as the sum of transit times for each sequential interbranch segment

$$TT(f) \sim \Sigma_i(V[i]/F[i]) = 0.308*f + 0.011 \text{ msec}, \quad (5)$$

where f is the fractional distance from epicardium to endocardium [9]. Figure 2, left panel shows the epi to endo-cardial trans-myocardial distribution of TT.

Transmural spatial distribution of intra-myocardial compression and impact on regional myocardial perfusion.

The myocardium has muscle fiber groups that are arranged in layers around the circumference of the left ventricular chamber's short axis [15]. Contraction of the muscle fibers should result in circumferential shortening with resulting decrease of the ventricular luminal (Ri) and epicardial surface (Ro) diameters. During contraction of these myocardial fiber layers the pressure in the myocardial wall increases until the aortic valve opens and the ventricular chamber empties into the aorta. The compressive force within the left ventricular myocardial wall is described by Lame's Law which links the transmural compressive pressure distribution $S_c(r)$, at radius r from center of a spherical, thick-walled container, subjected to transmural pressure P (chamber pressure = P, outside pressure = 0) and of inner surface (endocardial) radius R_i and outer surface (epicardial) radius R_o [8].

$$S_t(r) = P\{R_i^2/(R_o^2 - R_i^2)\}\{(1 - R_o^2/r^2)\} \quad (6)$$

See Figure 3 for schematic showing relationships of these radii. This relationship indicates the compressive force at the inner surface at r=Ri equals P, the pressure in the container (assume pressure on epicardium is zero [16]) and that the pressure P decreases progressively as location (r) within the wall at the epicardial surface of the myocardium equals the pressure at the outside of the myocardial wall. This distribution of transmural

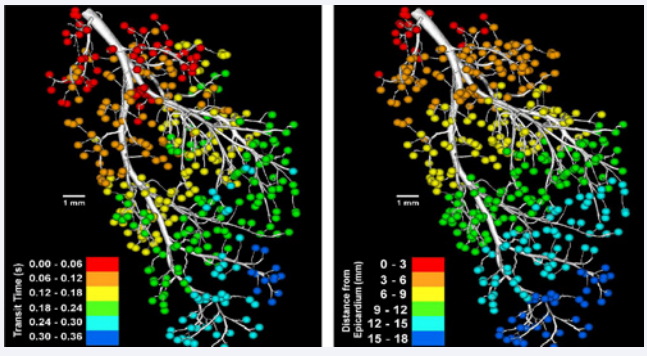

Figure 2 Micro-CT images of the same intramural arteriole. Epicardial origin left upper and distal terminus in right lower corner of each panel. The colored spheres added at the end of each terminal arteriole are coded. *LEFT* panel codes for computed blood flow transit time of blood flow from epicardial origin down to terminal arteriole. *RIGHT* panel codes for fractional distance (epi to endo-cardium) of each terminal arteriole.

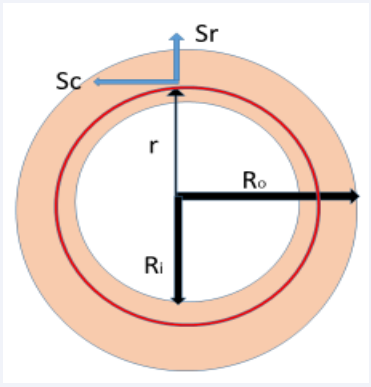

Figure 3 Schematic of left ventricular cross section showing radii used to calculate circumferential and transmural intra-myocardial stresses.

pressure has been confirmed by direct measurement to show sub-epicardial pressure at 0.2P and sub-endocardial pressure at 0.9P, where P is left ventricular chamber pressure [17].

An additional factor affecting the balance of regional myocardial perfusion would be any regional differences in myocardial work performed during myocardial contraction [**7**]. If we assume that the metabolic rate of myocardium during diastole, when no mechanical work is performed by the myocardium is the same in all intramural regions, the work performed during contraction should be proportional to circumferential tension (St) x shortening (δC) x duration of contraction (T) x number of heart cycles per minute (HR), where δCr is the decrease in regional circumference within the myocardial wall at distance r from the center of the LV chamber.

Circumferential tension, at intramural location at radius r within the wall, measured from the center of the LV chamber, is also described by Lame's Law [8] as follows:

$$Sc = P[Ri^2/(Ro^2 - Ri^2)]\,[1 + Ro^2/r^2] \quad (7)$$

The regional shortening $\delta Cr = 2\pi(rd - rs)$

where: rd is radial location at end diastole and rs is the radial location at end systole.

The work performed by the myocardium is estimated as the local circumferential tension (as per Equation 6) multiplied by the regional circumferential shortening.

If W(r) is the work performed at intramyocardial radius r and circumferential tension at r is Sc(r)(r)

$W(r) \sim Sc(r)(\,2\pi(rd\text{-}rs)$

At r=1 at the endocardium and r=2 and 1.85 at the epicardium the circumferential shortening from end-diastole to end-systole respectively equals (4π – 3.70 π) cm, ie ΔCr = 0.9425 cm and at the sub endocardium equals (π – 0.71π) cm, so that ΔCr = 0.9111 cm at the sub-endocardium. The average circumferential tension at the outer third of the epicardial myocardium is 0.219 units and in the sub-endocardial third is 0.913 units (normalized to 0.1 for left ventricular chamber pressure) so that the work (ie force x distance moved) performed at the sub-epicardium is 0.894 work units and in the sub-endocardium is 0.792 work units, ie essentially equal. This suggests that oxygen consumption (ie perfusion delivery) requirements are somewhat more than ten percent less in the subepicardial myocardium.

Interplay of the myocardial electro-mechanical activation, contraction and perfusion sequences within a single cardiac cycle

The myocardium is a syncytium of myofibers [18]. Consequently electrical activity in one location in the myocardium ultimately propagates throughout the myocardium. A branching network of Purkinje fibers convey an action potential to the endocardial myocardium, which then results in a wave of activation of the myocardium progressing from endocardium to epicardium at a velocity of 4mm/sec from endocardium to epicardium, ie completed activation within 63 msec [19]. Once an action potential activates a myocyte it contracts after about 8 msec [20]. Once the entire myocardium contracts it quickly builds up pressure in the left ventricular chamber until the pressure in the aorta is exceeded and then ejects the blood into the aorta, resulting in thickening of the myocardium.

Once the aortic valve opens the blood pressure in the epicardial coronary arteries follows essentially the same pressure-time profile as occurs in the ventricular chamber until the valve closes following which it remains higher than the pressure in the left ventricular chamber.

Once electrically activated, local myocardial contraction is maintained over a subsequent 0.2 to 0.3 seconds [21], depending on heart rate (294 msec at 90 BPM and 220 msec at 120 BPM) and magnitude of sympathetic activity [22,23]. The onset and duration of the ventricular isovolumic and subsequent ejection phases depends on the aortic blood pressure.

The following is the time-sequence of these events starting at end-diastole with left ventricular chamber pressure at 0 - 10 cm water and pericardial pressure at -8 to -1 cm water [16].

a) The progression of myocardial contraction from endo to epicardium results in a squeegee-like effect causing arrest and even reversal of blood flow within the intramural arteriolar tree, depending on the transmural compressive pressure distribution as described by Lame's Law [8].

b) Lame's Law (Equation 6) indicates that flow should be arrested where local intramural compression exceeds local arteriolar intraluminal blood pressure. Direct animal experiments also show such transmural flow distribution [24]. The pressure in capillaries is about 30 mmHg [25,26], so Equation 6 predicts that there is no capillary perfusion in the sub-endocardial region of the wall over the 0.2-0.3 seconds during systolic contraction. As the local intramural compressive pressure exceeds the approximately 30 – 40 mmHg pressure needed to maintain flow the blood flow has been observed to reverse during this period [27]. Simultaneously the volume of the compressed wall decreases at a rate of 4.7 – 6.8 ml/g/min at the epicardium and 10.8 ml/g/min at the sub-endocardium due to the transiently reduced intravascular blood volume [28].

c) Once the left ventricular pressure decays after start of relaxation of the myocardium the intramural compressive force also decreases to the point that blood flow can resume in the previously compressed arterioles [27,28]. However, based on computed transit time of blood flow along the intramyocardial arterioles, the return of blood flow to the sub-endocardium could take as much as 0.3 seconds in a one cm thick wall and proportionally less closer to the epicardium [9]. Due to the intramural pressure distribution the myocardium close to the epicardium might continue to be perfused throughout myocardial contraction.

d) The effect of heart rate is largely governed by the length of time remaining in the cardiac cycle after cessation of myocardial contraction as illustrated schematically in (Figure 4) [29]. Thus at a heart rate of 60 BPM the maximum time available for return of perfusion is 1.0 – 0.3 =0.7 seconds at the sub-endocardium and at 120 BPM this changes to 0.5-0.3 = 0.2 seconds. Thus the fraction of a heart cycle that allows for sub-endocardial perfusion decreases markedly with increased heart rate. This no-flow period is actually lengthened somewhat by the extra time needed to refill the downstream arteriole before tissue perfusion can start. The duration of this added no-perfusion period depends on the transit time (TT) from the location in the sub-epicardium that is not perfused to the distal arterioles, which could be as long as an additional 0.3 seconds at the very sub-endocardium. The fact that in the resting state sub-endocardial blood flow is elevated relative to that in the sub-epicardial region now compensates for the reduced time available for perfusion in the sub-endocardium. Figure 5 graphically show how the interaction between these factors results in the average perfusion at various locations between the epicardium and endocardium. In the normal heart increasing heart rate is usually associated with increased myocardial perfusion reserve can be as much as five-fold that under resting heart rate conditions [27,5]. This analysis of myocardial perfusion is based on the assumption that the terminal arteriolar diameters are under resting conditions. However there are several mechanisms that control arteriolar diameter in response to exercise and other physiological stress conditions. Those mechanisms are assumed to provide the flow reserve which we apply in proportion to heart rate [30].

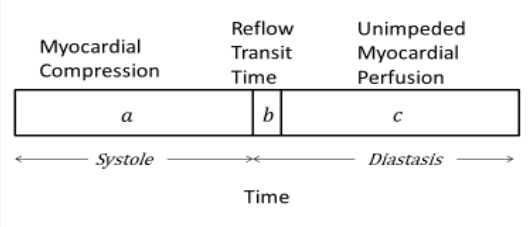

Figure 4 Schematic representation of the time sequence of one generic cardiac cycle. The magnitude of perfusion reserve invoked during each cardiac cycle depends on metabolic demand. The three phases are of the cardiac cycle are systolic contraction (a), delayed reperfusion of the myocardium due to the location-dependent transit time of reperfusion of the intra-myocardial arteriolar tree (b) and diastacis when unimpeded perfusion can occur (c). The duration of each of these phases changes with heart rate (ie cycle length). The perfusion duty cycle for each heart cycle equals (duration of Phase c)/ (duration of Phases a+b+c).

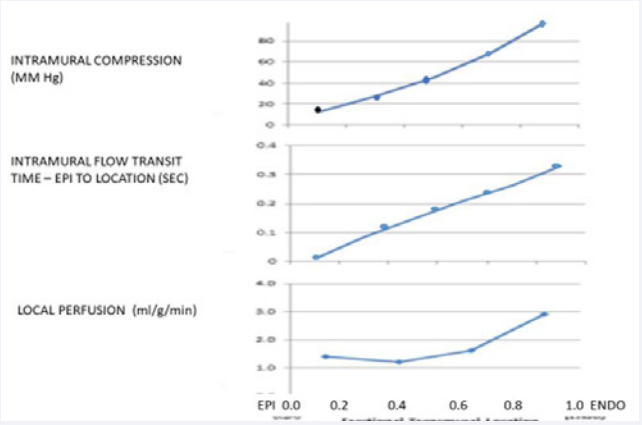

Figure 5 All three panels show data, at transmural locations, that are responsible for the intra-myocardial perfusion duty cycle. *Upper panel* shows local intra-myocardial compression pressure based on Lame's Law. *Middle panel* shows flow transit time along paths from epicardial origin to terminal arterioles at the various transmural locations. *Lower pane*l shows myocardial perfusion estimates (assuming perfusion throughout the entire cardiac cycle) computed from myocardial micro-CT images of insitu intra-myocardial terminal arterioles based on data generated in another study [9].

SUMMARY AND CONCLUSIONS

Experimentally demonstrated reduction of sub-endocardial perfusion relative to sub-epicardial myocardial perfusion during increase in heart rate is to be expected from the combination of effects of the branching geometry of the intramural arteriolar trees, the distribution of intra-myocardial stresses during myocardial contraction, the shortening of the transmural difference in the duration available for myocardial perfusion relative to shorter cardiac cycle and the reduced duration of sub-endocardial perfusion as compared to the duration of sub-epicardial perfusion. The reduction of intra-coronary arterial pressure, distal to a stenosis, would accentuate these physiological effects and thereby preferentially compromise sub-endocardial perfusion.

ACKNOWLEDGEMENTS

This work uses data generated in part by National Institutes of Health grant R021 HL-117359.

REFERENCES

1. Ball RM, RJ Bache, FR Cosbb, JC Greenfield Jr. Regional myocardial blood flow during graded treadmill exercise in dogs. J Clin Invest. 1975; 55: 43-49.

2. Falsetti, RJ Carroll, ML Marcus. Temporal heterogeneity of myocardial blood flow in anesthetized dogs. Circulation. 1975; 52: 848-853.

3. Larghat A, J Biglands, N Maredia, JP Greenwood, SG Ball, M Jerosch-Herold, et al. Endocardial and epicardial myocardial perfusion

determined by semi-quantitative and quantitative myocardial perfusion magnetic resonance. Int Jnl Cardiovascular Imaging. 2012; 28: 1499-151.

4. Levine HD, Ford RV. Subendocardial Infarction: Report of six cases and critical survey of the literature. American Heart Journal. 1950; 1: 246-263.

5. Hoffman JIE, Buckberg GD. Pathology of subendocardial ischaemia. Br Med J. 1975; 1: 76-79.

6. Canty Jr, Klocke FJ. Reduced regional myocardial perfusion in the presence of pharmacologic vasodilator reserve. Circulation. 1985; 71: 370-377.

7. Suga H. Cardiac Energetics: From Emax To Pressure-Volume Area. Clinical and Experimental Pharmacology and Physiology. 2003; 30: 1440-1681.

8. DenHartog J P. Strength of materials, Dover Publisher New York. 1949; 143.

9. Ritman EL,Vercnocke AJ, Zamir M. Probing the depths of the myocardium: vasculature, Transit time and perfusion within the left ventricular wall. Ann Biomed Eng. 2019; 47: 1281-1290.

10. Zamir M. Distributing and delivering vessels in the human heart. J Gen Physiol. 1988; 91: 723-735.

11. Wieringa PA, HG Stassen, JD Laird, JA Spaan. Quantification of arteriolar density and embolization by microspheres in rat myocardium. Am J Physiol. 1988; 4: H636-H650.

12. Wearn JT, Mettier SR, Klumpp TG, Zschiesche LJ. The nature of the vascular communicants between the coronary arteries and the chambers of the heart. Am Heart J. 1933; 9: 143-164.

13. Mayrovitz HN, J Roy. Microvascular blood flow: evidence indicates a cubic dependence on arteriolar diameter. Am J Physiol. 1983; 245: H1031-H103.

14. Sutera SP, R Skalak. The history of Poiseuille's Law. Annual Review of Fluid motion. 1993; 25: 1-29.

15. Streeter DD Jr, Spotnitz HM, Patel DP, Ross J Jr, Sonnenblick EH. Fiber orientation in the canine left ventricle during diastole and systole. Circ Res. 1969; 24: 339-347.

16. Kenner HH, EH wood. Intrapericardial, intrapleural and intracardiac pressures during acute heart failure in dogs studied without thoracotomy. Circ Res. 1966; 19: 1071-1079.

17. Heineman FW, Grayson J. Transmural distribution of intramural pressure measured by micropipette technique. Am Jnl Physiol. 1985; 249: H1216- H1223.

18. Faroalk DW, Selby CC. Observations on the fine structure of the turtle atrium. J Biophys Biochem Cytol. 1958; 4: 63-72.

19. Durrer D, R Th Van Dam, GE Freud, MJ Janse, FL Meijler. C Arzbaecher. Total Excitation of the isolated human heart. Circulation. 1970; 41: 899-912.

20. Wyman BT, WC Hunter, FW Prinzen, ER McVeigh. Mapping propagation of mechanical activation in the paced heart with MRI imaging. Am J Physiol. 1999; 276: H881-H891.

21. Golde D, L Burstin. Systolic Phases of the cardiac cycle in children. Circulation. 1970; 42: 1029-1036.

22. Ferro G, Ricciardelli B, Sacca L, Chiariello M, Volpe M, Tari MG, et al. Relationship between systolic time intervals and heart rate during atrial ventricular pacing in normal subjects. Jpn Heart J. 1980; 21: 765-771.

23. Hurst JW, Logue. The Heart, 2nd Edition McGraw-Hill New York. 1970; 76.

24. Hess DS, Bache RJ. Transmural distribution of Myocardial blood flow during systole in the awake dog. Circ Res. 1976; 38: 5-15.

25. Bellamy RF. Diastolic coronary flow relationships in the dog. Circ Res. 1978; 43: 1978, 92-101.

26. Jones CJH, L Kuo, MJ Davis, WM Chilian. Regulation of coronary blood flow: coordination of heterogeneous control mechanisms in vasomotor microdomains. Cardiovascular research. 1995; 29: 585-596.

27. Toyota E, Y Ogasawara, O Hiramatsu, H Tachibana, F Kajiya, S Yamamori, et al. Dynamic flow velocities in endocardial and epicardial coronary arteries. Am J Physiol. 2005; 288: 4.

28. Ashikaga H, BA Coppola, KNG Yamazaki, FJ Villarreal, JH Omens, JW Covell. Changes in regional myocardial volume during the cardiac cycle: implications for transmural blood flow and cardiac function. Am J Physiol. 2008; 295: H610-H618.

29. Fokkema DS, JW GE Van Teeffelen, S Dekker, E Vergroesen, JB Reitsma, et al. Diastolic time fraction as a determinant of subendocardial perfusion. Am J Physiol. 2005; 288: H2450-H2456.

30. Grattan MT, Hanley FL, Stevens MB, Hoffman JIE. Transmural coronary flow reserve patterns in dogs. Am J Physiol. 1986; H276-H283.

Cite this article

Ritman EL (2022) Intra-Myocardial Arteriolar Architecture Impact on Vulnerability of Sub-Endocardium to Ischemia. Ann Vasc Med Res 9(2): 1145.